Werk

Jahr: 1977
Kollektion: fid.geo
Signatur: 8 Z NAT 2148:
Digitalisiert: Niedersächsische Staats- und Universitätsbibliothek Göttingen
Werk Id: PPN1015067948_0043
PURL: http://resolver.sub.uni-goettingen.de/purl?PPN1015067948_0043

LOG Id: LOG_0041
LOG Titel: The upper mantle under western Europe inferred from the disperion of Rayleigh modes
LOG Typ: article

Übergeordnetes Werk

Werk Id: PPN1015067948
PURL: http://resolver.sub.uni-goettingen.de/purl?PPN1015067948
OPAC: http://opac.sub.uni-goettingen.de/DB=1/PPN?PPN=1015067948

Contact

Niedersächsische Staats- und Universitätsbibliothek Göttingen
Georg-August-Universität Göttingen
Platz der Göttinger Sieben 1
37073 Göttingen
Germany
Email: gdz@sub.uni-goettingen.de

J. Geophys. 43, 265–285, 1977

Journal of Geophysics

The Upper Mantle under Western Europe Inferred from the Dispersion of Rayleigh Modes

Guust Nolet

Vening Meinesz Laboratory, Lucas Bolwerk 6, Utrecht, The Netherlands

Great waves looked over others coming in
And thought of doing something to the shore
That water never did to land before.
Robert Frost

Abstract. A stacking technique is applied to measure phase velocities of the fundamental and several higher Rayleigh modes over an array of long period stations located in Western Europe. The higher mode dispersion has been measured for periods between 25 and 100 s and for phase velocities up to 7.5 km/s.

Using Backus-Gilbert inversion, a detailed model for the shear wave velocity in the upper mantle under the array is obtained. The low velocity zone is located between 150 and 230 km depth and is not very pronounced, but it is preceded by a rise in S velocity around 120 km depth. Strong velocity gradients are found at depths of 360 and 520 km. A good fit to the data can only be obtained if a zone of low density is assumed at a depth of 220 km or there about. As yet little can be said about depth, shape and extent of this zone, but the magnitude of the density drop implies a chemical or mineralogical stratification. A mechanism based on eclogite fractionation (Press, 1969) appears to be a likely candidate as the cause for such a gravitationally unstable stratification.

Key words: Europe – Higher modes – Rayleigh waves – Upper mantle.

1. Introduction

Most of the information that we now have about the shear wave velocity in the lithosphere and asthenosphere has been derived from surface wave dispersion measurements. Since the installation of the standard station network (W.W.S.S.N.) and the development of fast and accurate numerical methods for

data-processing (see Dziewonski and Hales, 1972, for a review), the number of regional studies using surface wave dispersion has grown considerably. The observational material has mainly been limited to the fundamental mode of Love and Rayleigh waves. These data are very useful for a probing of the depth of the lithosphere, can be used to establish the existence of a low velocity zône (LVZ) and make a subdivision of the earth in regions of different character possible (Knopoff, 1972). However, detail in the asthenosphere is not resolvable (Seidl, 1971) and the depth to which the LVZ extends is poorly determined.

It has long been argued that the observation of long period higher modes should add information about the earth's interior that is distinctly new compared to the knowledge that can be obtained from observation of the fundamental modes only. Wiggins (1972) and Der and Landisman (1972) substantiate these claims numerically for the first few higher modes using resolution analysis of the Backus-Gilbert type.

To illustrate the gain in resolution for the shear velocity that is obtained if a large number of higher mode phase velocities are measured, I have calculated the resolving power of 7 different data sets. The first data set consists of the fundamental Rayleigh mode curve, at periods corresponding to waves with horizontal wavelengths between 130 and 600 km. The second data set consists of the same fundamental mode curve plus one for the first higher Rayleigh mode, in the same wavelength interval. The data set is extended in the same manner with the second mode, and so on. All these hypothetical phase velocity data are assumed to have a precision of 0.5 % and for all sets the resolving power was calculated.

According to Backus and Gilbert (1970), the length scale of the detail which a given data set can resolve at a particular depth is a function of the error that we allow in the solution to the linearized inverse problem. The results of the calculation for 2 different values of this model error ε are condensed in Figure 1. The addition of the first higher mode greatly enhances the resolution in the LVZ, and introduces some resolution at deeper levels where the fundamental mode does not reach. Addition of the 2nd and 3rd mode emphasizes this effect but the gain in resolution is by far not so dramatic when the data set is enlarged with modes 4 and higher.

Although the rather low errors assumed in calculating these resolutions will not easily be reached for higher modes, we may conclude from Figure 1 that it is highly desirable to extend local measurements of fundamental mode disperion with similar data for the higher modes.

In the past 20 years a great number of higher mode group velocity measurements have been made, especially for impulsive waves like Li, Lg and Sa. See Kovach (1965) and Alterman (1969) for reviews. In general, however, these data are not usable for inversion because it is impossible to identify the exact mode number of the dispersed wavetrain, due to the overlap in the higher mode group velocity curves. Furthermore, any identification is probably dependend on the theoretical model since group velocities may vary strongly for different models. Phase velocity measurements might be identified with less uncertainty but are almost impossible to observe in one record because of the mutual interference of different modes. However, Crampin (1964) succeeded in obtaining phase velocity

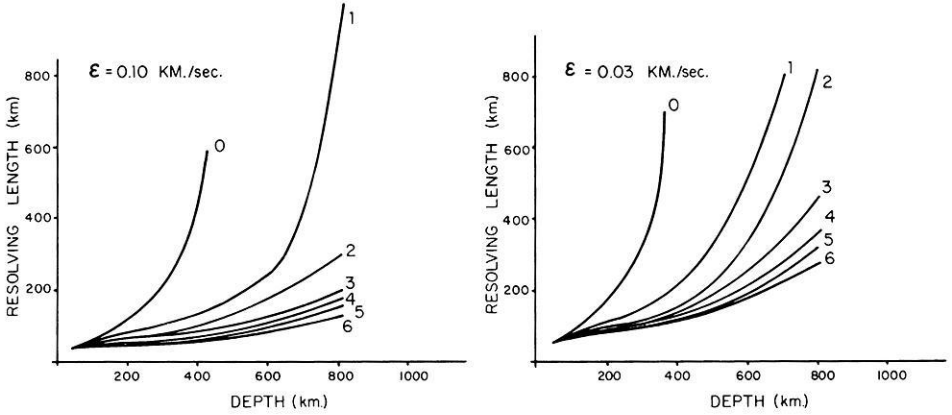

Fig. 1. Reduction of the resolving length for the shear wave velocity with the addition of higher Rayleigh modes, is shown as a function of depth for two values of the model error ε. Numbers denote the highest mode number present in the data set

curves for the first higher Rayleigh mode at periods below 13 s using the peak and trough method.

Recently, several attempts to measure clearly identified higher modes have been successful. Nolet (1975) employs a stacking technique with an array of standard long period station to obtain the average phase velocities of a number of Rayleigh modes over Western Europe in the period range of 20–100 s, while Forsyth (1975) uses several events and several stations to determine those phase velocities of the fundamental and first higher Love mode that best fit the observed phases in a least-squares sense over an oceanic path.

Earlier, Mendiguren (1973) and Gilbert and Dziewonski (1975) used the W.W.S.S.N. stations as a network to identify higher modes in the period range of the earth's eigenfrequencies ($T > 80$ s).

Nolet and Panza (1976) modified the stacking technique to include a deconvolution algorithm for a better identification of the modes and tested the method using a synthetic seismogram. This paper is a first attempt to obtain a precise estimate of higher Rayleigh mode phase velocities using the new method and interprete these data in terms of a model for the upper mantle.

2. The Stacking Method

In this section I briefly review the principles of the stacking technique. For more detail the reader is referred to Nolet and Panza (1976).

If $w(\Delta, \omega)$ denotes the spectrum of the signal $u(\Delta, t)$ in a station at Δ km from the source, then an estimate for the wave-number spectrum can be obtained by means of stacking:

$$\hat{W}(k, \omega) = \frac{1}{N} \sum_j w(\Delta_j, \omega)\, e^{-ik\Delta_j}. \tag{1}$$

The spectrum of a component of the signal in station j can be represented by (Nolet, 1976):

$$w\ (\Delta_j, \omega) = \sum_n F_{nj}(\omega)\ \exp\{i[k_n(\omega)\,\Delta_j + \phi_{nj}(\omega)]\} \tag{2}$$

where n is the mode number, which is 0 for the fundamental mode, $F_{nj}(\omega)$ the amplitude spectrum in station j and $k_n(\omega)$ the wave-number of mode n. $\phi_{nj}(\omega)$ is the initial phase.

In general, ϕ is only weakly dependend on azimuth and we may neglect the variations of $\phi_{nj}(\omega)$ in the different stations. We can usually make an approximate but fairly good correction for the effects of damping and geometrical spreading by equalizing the energy of the signals in all the stations. Thus, we can remove the subscript j from F and ϕ and find from (1) and (2):

$$\hat{W}(k, \omega) = \sum_n F_n(\omega)\ \exp\{i\,\phi_n(\omega)\}\ H\{k_n(\omega) - k\} \tag{3}$$

where

$$H(k) = \frac{1}{N} \sum_i \exp(ik\Delta_i). \tag{4}$$

$|H(k)|^2$ is called the array response, which is 1 in $k=0$. For an ideal array it should resemble a δ-function. $|\hat{W}(k, \omega)|^2$ will then have sharp maxima in curves (k, ω) that are parametrized by the dispersion relation $\omega = \omega_n(k)$, which is the datum that we want to measure. In practice the sidelobes of $H(k)$ disturb this simple picture. To minimize the influence of sidelobes 2 modifications are made to the above scheme:

(a) We split each signal into a number of segments around arrival times determined by a series of group velocities U. This reduces the number of modes in the stack. The stack now depends on the group velocity U. At a fixed value of ω we display $|\hat{W}(k, \omega)|^2$ in a plane of U vs k, which is called a mode-separation diagram. This approach has also been proposed by Cara (1976).

(b) Since we know the shape of $H(k)$ we could remove the side-lobes if we knew where its central peak is located. Assuming that the largest maximum of $\hat{W}^2$ in each column of the separation diagram coincides exactly with this main lobe, this is what we in fact try to do in an iterative scheme called "cleaning". This process leads to a less ambiguous interpretation of complicated responses and to better phase velocity determination for modes that are not dominant in amplitude.

3. Description of the Data-Set

Western Europe is a favourable location for an application of the method outlined above. It has a quite high density of long period stations (both national and W.W.S.S.N. stations are used), and the Eurasian continent is so large that earthquake waves can travel 10,000 km without crossing an ocean/continent boundary. This optimizes the temporal separation of the higher modes without introducing strong refraction along the wave paths. In general the preferred source location was near Japan and the Kurile Islands region since the direction of arrival of these events enables us to profit most from the full length of the

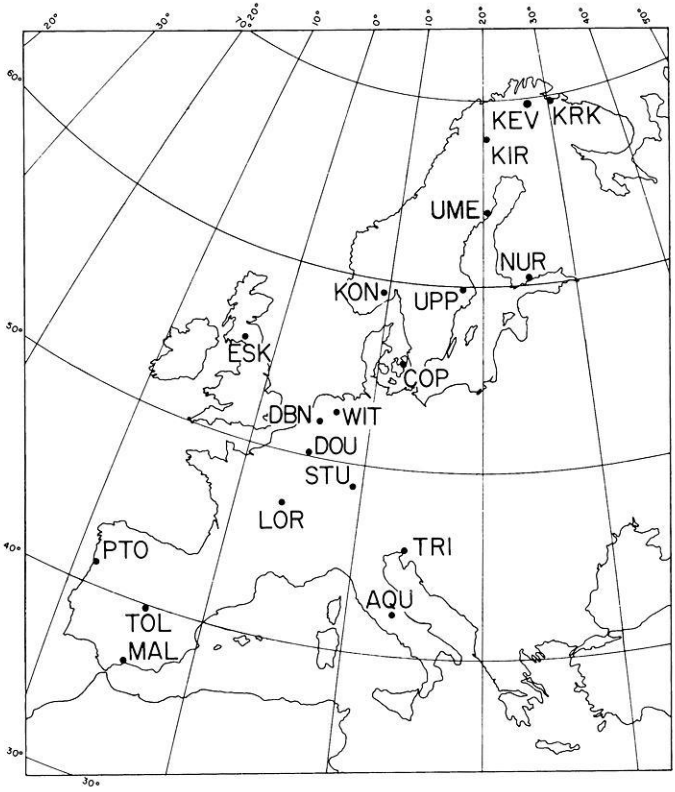

Fig. 2. The network of long period stations

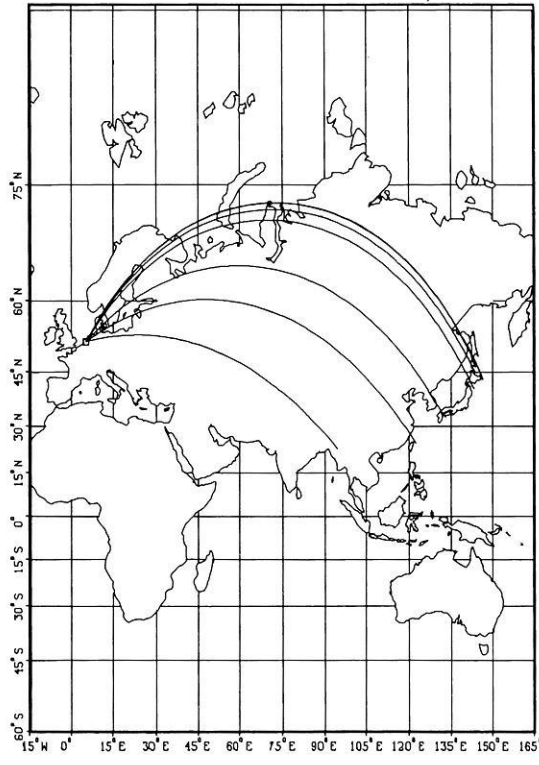

Fig. 3. Great circle paths from the epicentres to station De Bilt (DBN). The paths to events 3 and 6, both located in Hokkaido, coincide

Table 1. Listing of events (ISC estimates)

No.	Date	Origin time	Latitude	Longitude	Region	Depth	m_b	N
1	23-06-64	$1^h26^m36.8$	43.16 N	146.17 E	Kurile Isl.	76	6.4	11
2	29-03-65	$10^h47^m38.4$	40.73 N	142.85 E	Honshu	41	6.1	16
3	25-10-65	$22^h34^m22.4$	44.21 N	145.45 E	Hokkaido	159	6.1	12
4	01-07-66	$5^h50^m38.0$	24.86 N	122.56 E	Taiwan	102	6.1	12
5	05-08-68	$16^h17^m05.5$	33.31 N	132.31 E	Shikoku	48	6.2	9
6	10-01-69	$7^h02^m07.9$	44.89 N	143.21 E	Hokkaido	238	6.3	13
7	17-10-69	$1^h25^m11.5$	23.09 N	94.70 E	Burma	124	6.1	14

array, as can be seen in Figures 2 and 3. Since the mutual interference of modes is a strong function of their excitation it was attempted to obtain a large variety of source depths, even if this meant that events from less suitable locations (Taiwan, Burma) had to be chosen. The 7 events that were selected for processing are listed in Table 1, where N denotes the number of recordings used.

The vertical components of the recordings were digitized on a semi-automatic digitizer with an interval usually less than 1 second. As small timing errors introduce large errors in the phases a program was written to correct the digitized records for small irregularities in the drum speed and photographic distortions of the print. The time accuracy is believed to be better than 2 seconds for recordingings at fast drum speed (30 mm/min) and a little worse for recordings at a speed of 15 mm/min. Digitization usually started with the onset of the S-pulse and continued at least to a time corresponding to a group velocity of 4.0 km/s.

4. Observation of Higher Modes

Each of these 7 events was stacked and analysed for 13 different periods ranging from 25.6 to 102.4 s, using the stacking method. Figure 4 shows the results for event nr. 3. For this event the stations are regularly distributed along the Δ-axis and the source is in line with the array axis. It is an example of a "good" data set. Figure 5 shows how the mode-separation may deteriorate if the stations are less evenly distributed, the station azimuths differ considerably and the great-circle paths cross slightly different geological provinces (event 4). There is enough coherence however to resolve the higher modes.

The crosses in Figures 4 and 5 denote the theoretical locations of the modes calculated for the Gutenberg-Bullen A continental model, and correspond to the numbers to the right of each figure. These theoretical values are used for identification only. Numbers in the right hand upper corner denote the period in seconds. The group velocity is given in km/s. Contours show the dB level down from the maximum value. The contour interval may be 1 or 2 dB. The number of contours is limited to 5. Hence, when the energy at a certain group velocity interval dominates the rest of the signal, the remaining part of the diagram may lack detail. This short-coming does not exist in the printer versions of the diagrams.

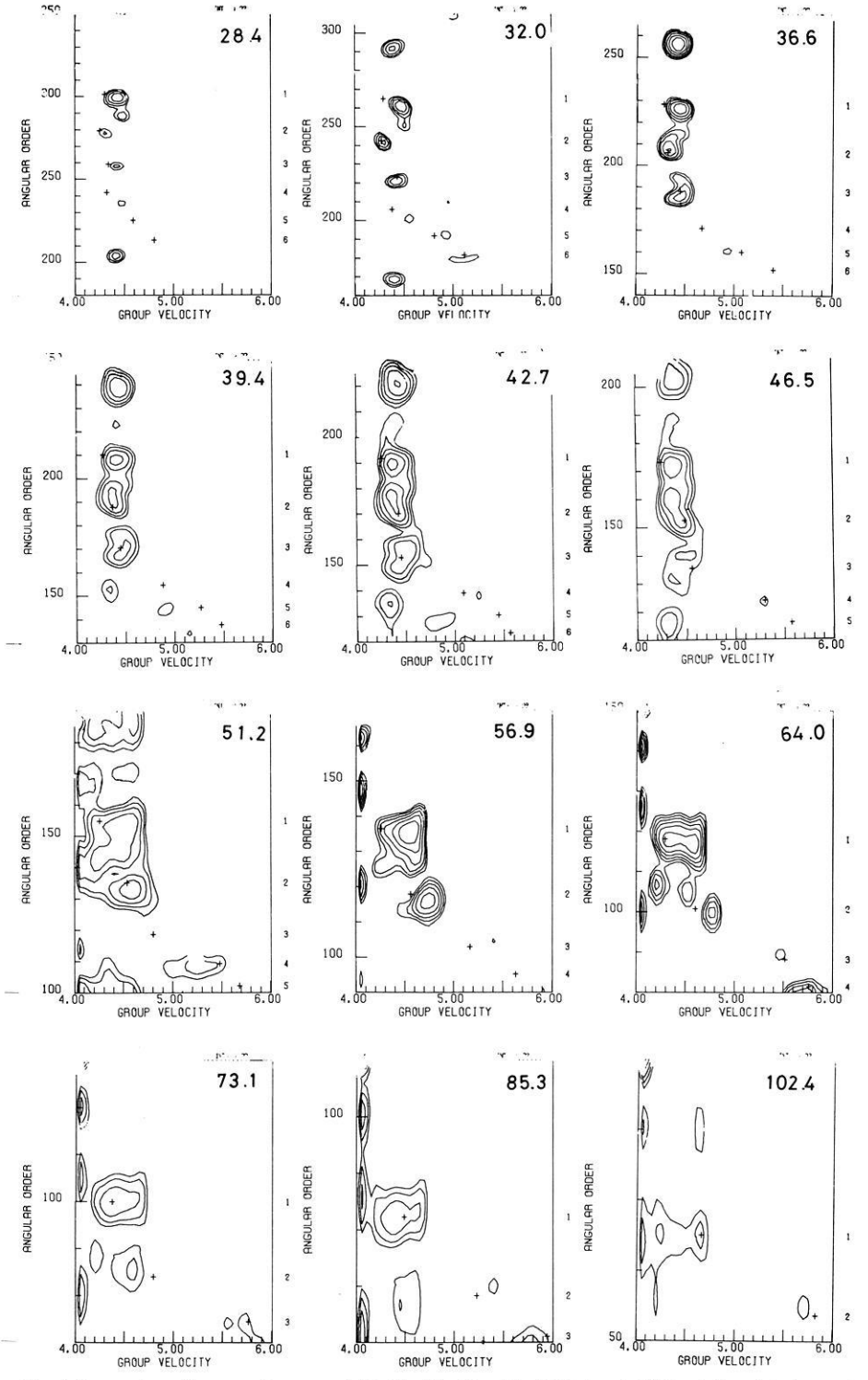

Fig. 4. Separation diagrams for event 3 (Hokkaido, Oct. 25, 1965, depth 159 km). For details see text

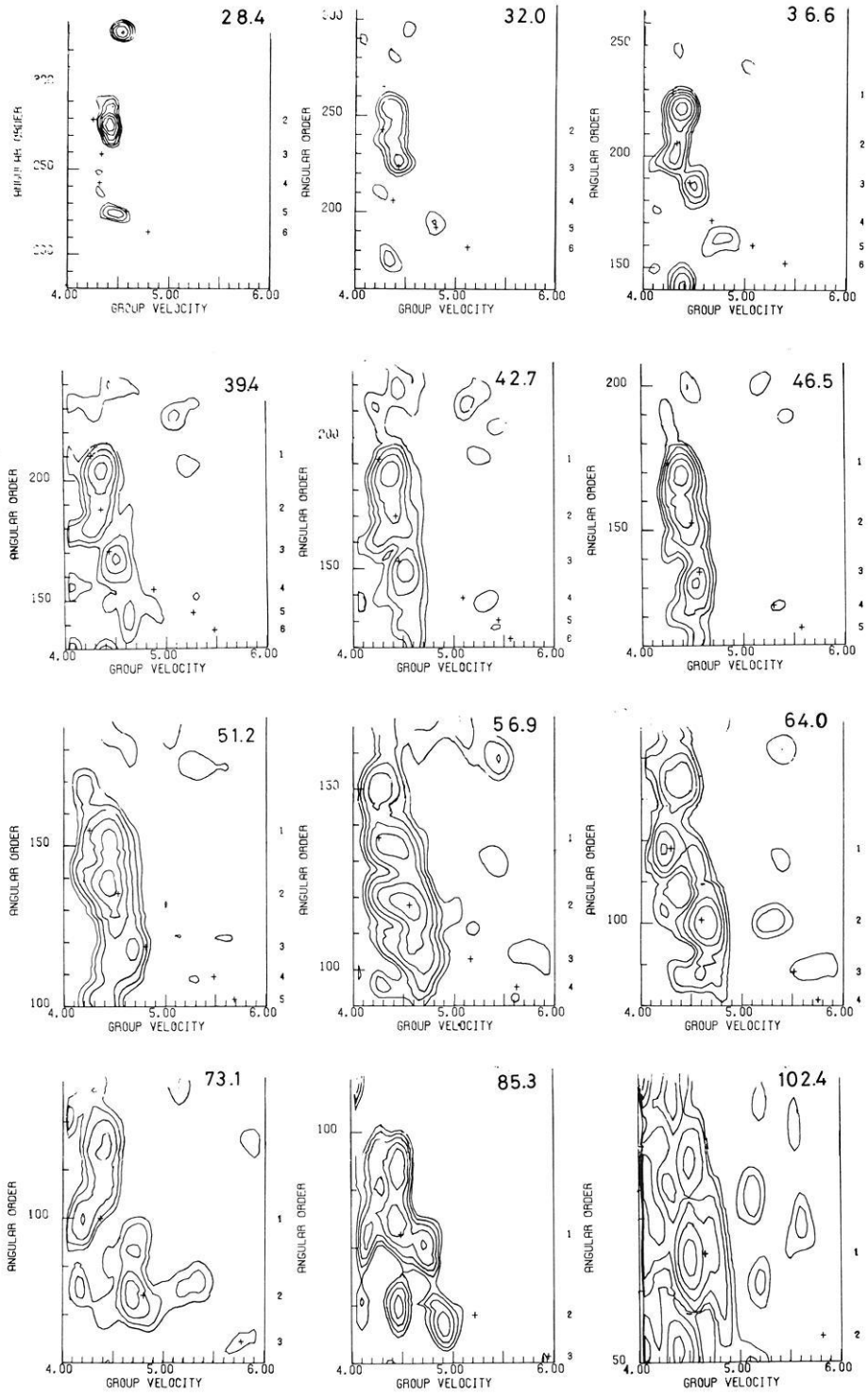

Fig. 5. Separation diagrams for event 4 (Taiwan, July 1, 1966, depth 102 km). For details see text

In the separation diagrams there are often more maxima present than would be expected if the signal consisted only of a few Rayleigh modes and if the signal could be perfectly resolved using the cleaning algorithm. This is due to a number of reasons:

(a) Errors in the digitizations, instrument calibration and source location.

(b) Approximations in the theory like the neglect of initial phase and damping.

(c) Disturbing effects from core-reflected body waves or from very high modes, that arrive in the same time-interval.

(d) Refracted or reflected arrivals due to lateral inhomogeneity.

(a) and (b) will not only shift the maximum of a higher mode from its true value, they will also disturb the cleaning process by broadening of the peaks, so that sidelobes will not be removed effectively.

(c) and (d) will cause other maxima in the field that do not belong to sidelobes of the first few higher mode spectral peaks. These are not removed by the cleaning algorithm.

(d) is probably not important for the higher modes under study, which have most of their energy below the lithosphere. Since the fundamental mode shows a high degree of coherency over the array-area at periods larger than about 35 s, most of the large-scale lateral hetergeneity along the source-station paths should be confined to the upper 120 km. (c) can be of considerable influence, as it is in event 1.

The misidentification of false peaks as true modes is a severe source of error (Nolet and Panza, 1976). The situation is not unlike that of the early normal mode spectra, and misidentifications are bound to occur. Since the 7 events are all of a completely different character one may hope that the net effect of errors and misidentifications is only small in the average values found for the phase velocities.

Since group velocity measurements with this method may contain large errors, they are not used for the inversion. The group velocity data are nevertheless very useful for the identification of the modes: if a group velocity for one of the events is significantly off compared to the other events the reading is rejected. Sometimes a rejected reading could be replaced by a second maximum of comparable magnitude that was in agreement with the other group velocities.

At the outset, 360 readings of phase and group velocities were made from 91 separation diagrams. With the group velocity criterion 40 of these readings were rejected without replacement, 33 were replaced by comparable maxima with a good group velocity fit.

The remaining data were plotted for each period in a phase velocity vs. group velocity plane (Fig. 6). If a cluster of readings for one mode was not clearly separated from the next mode all readings for both modes were rejected, since mode identification may be ambiguous.

Finally, average phase velocities have been calculated for each period. Assuming that the errors are normally distributed, standard errors have been calculated and a 99 % confidence interval has been assigned using student's t-distribution. 17 readings outside this interval have been rejected.

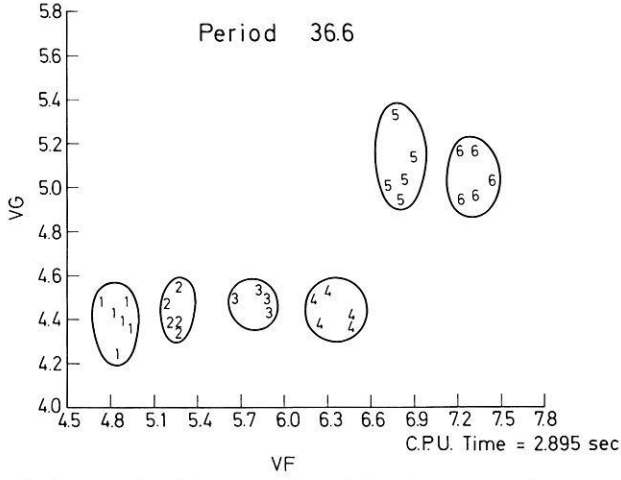

Fig. 6. Example of the separation of data in a plane of phase velocity (horizontal axis) vs. group velocity. For details see text

The phase velocities and their standard error are listed in Table 2. Most of the fundamental mode data in this table are taken from Nolet (1975). Two points, at 130 and 150 s have been taken from the path COP-MAL as measured by Seidl (1971). The individual higher mode phase velocity measurements and the average values of the fundamental mode are shown in Figure 7.

5. Inversion

Since the Backus-Gilbert method of inversion (Backus and Gilbert, 1970; Gilbert, 1971; Wiggins, 1972; Jackson, 1972) searches for the model correction to a starting model that is smallest in a least-squares sense, the choice of a starting model may be decisive for the final result, especially at those depth-ranges where the data only weakly constrain the model. Hence, care has to be taken in the construction of the starting model. On the other hand, as pointed out by Anderson and Hart (1976), this enables us to incorporate other types of data into the inversion scheme.

Some modes that have been measured reach to a depth of about 1500 km. However, their resolving power at this depth is very limited and the starting model is not likely to be changed significantly for depths larger than about 800 km. The earth's deep structure is well defined by the periods of free oscillations. On that account, model 1066 A (Gilbert and Dziewonski, 1975) was adopted as a starting model for depths greater than 420 km, since this model is based on a large number of eigenperiods, measured on a worldwide scale. Above this depth a smooth transition was made to the Gutenberg continental model since this had already proved its good fit to the fundamental mode measurements (Nolet, 1975).

Table 2. Rayleigh mode phase velocity

Period (s)	Phase velocity	Standard error	Model 7
Fundamental mode			
28.44	3.84	0.02	3.83
32.00	3.87	0.02	3.88
36.57	3.91	0.01	3.92
39.39	3.94	0.01	3.94
42.67	3.97	0.01	3.96
46.55	3.98	0.01	3.97
51.20	3.99	0.01	3.99
56.89	4.01	0.01	4.01
64.00	4.02	0.02	4.02
73.14	4.05	0.02	4.04
85.33	4.08	0.03	4.07
102.40	4.11	0.03	4.11
113.77	4.14	0.03	4.15
130.00	4.17	0.03	4.20
150.00	4.29	0.03	4.29
First higher mode			
28.44	4.69	0.02	4.70
32.00	4.79	0.03	4.76
36.57	4.86	0.03	4.83
39.39	4.88	0.05	4.88
42.67	4.94	0.03	4.93
46.55	5.03	0.02	5.00
51.20	5.09	0.01	5.08
56.89	5.17	0.03	5.18
64.00	5.31	0.01	5.30
73.14	5.51	0.01	5.45
85.33	5.73	0.07	5.66
102.40	6.02	0.13	5.97
Second higher mode			
25.60	4.92	0.02	4.96
28.44	5.03	0.04	5.04
32.00	5.17	0.01	5.15
36.57	5.26	0.02	5.29
39.39	5.31	0.04	5.37
42.67	5.40	0.05	5.47
46.55	5.53	0.03	5.60
51.20	5.72	0.05	5.75
56.89	5.92	0.06	5.95
64.00	6.19	0.04	6.21
73.14	6.48	0.03	6.53
Third higher mode			
25.60	5.27	0.06	5.29
32.00	5.64	0.05	5.56
36.57	5.82	0.07	5.76
39.39	5.98	0.05	5.90
42.67	6.11	0.06	6.07
46.55	6.34	0.07	6.28
51.20	6.59	0.05	6.52
56.89	6.87	0.05	6.79
64.00	7.03	0.04	7.07
73.14	7.35	0.02	7.36
Fourth higher mode			
32.00	5.97	0.02	6.02
36.57	6.34	0.07	6.30
39.39	6.47	0.02	6.48
42.67	6.68	0.01	6.68
51.20	7.17	0.05	7.18
56.89	7.44	0.01	7.43
Fifth higher mode			
28.44	6.20	0.08	6.17
32.00	6.45	0.03	6.46
36.57	6.81	0.04	6.84
39.39	7.06	0.02	7.05
42.67	7.29	0.03	7.25
Sixth higher mode			
25.60	6.40	0.07	6.30
28.44	6.57	0.04	6.57
32.00	6.92	0.05	6.89
36.57	7.30	0.06	7.25
39.39	7.43	0.08	7.43

For the upper 100 km the model gradually looses its significance since the lateral heterogeneity may become strong, especially in the crust. The Moho was fixed at 33 km depth on the basis of studies by Båth (1971), Payo (1965), Sapin and Prodehl (1973) and Seidl (1971). Only near the Alps is the Moho significantly deeper, but this region does not affect the data very much. Rather arbitrarily, the Conrad discontinuity in the starting model is placed at a depth of 20 km; the seismic velocities in the granitic (6.00, 3.46) and in the basaltic layer (6.70, 3.82) represent rough averages from the values found by the authors quoted.

The shear wave velocity directly under the Moho is 4.49 km/s in the starting model, on the basis of S_n velocities measured by Båth (1971), Fagerness and

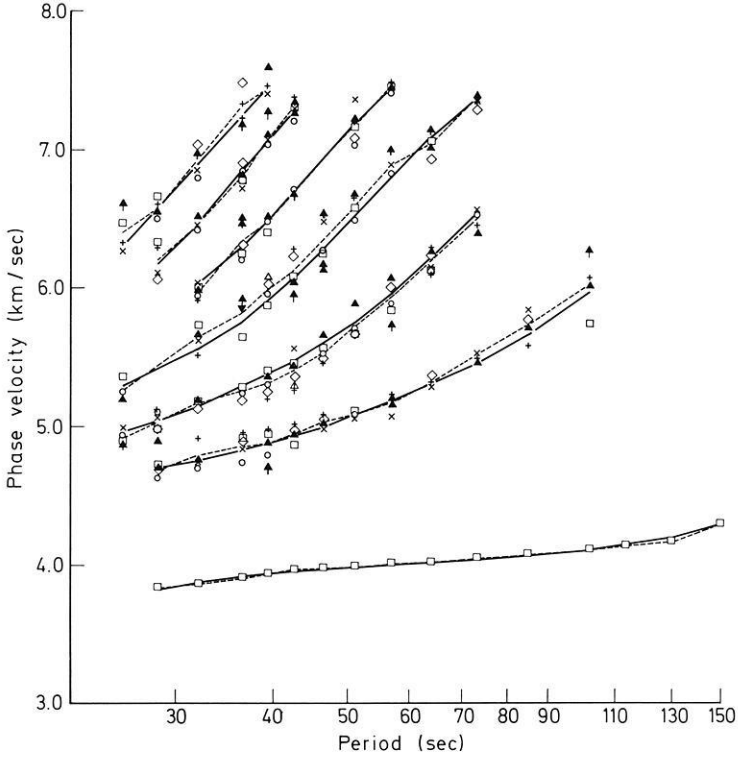

Fig. 7. Rayleigh wave phase velocity measurements over an array of stations in Western Europe for the 7 events listed in Table 1. The dashed lines connect the average values, the solid curves represent the theoretical values for model 7. The curve for the fundamental mode is at the bottom, the curves for 6 higher modes follow in order of increasing phase velocity

Kanestrom (1973) and Payo (1964). Their S_n values are somewhat lower than the 4.67 km/s reported by Lehmann (1961) and are not consistent with lid velocities of 4.6–4.7 km/s found by several surface wave studies (Payo, 1965; Seidl, 1971; Mayer Rosa and Mueller, 1973). The inversion performed in this paper shows, however, that a low lid-velocity can agree with the phase velocities of the fundamental Rayleigh mode.

The phase velocity data have first been inverted for the shear wave velocity only. This resulted in a rise in velocity near 120 km depth (4.52 km/s) and a not very pronounced LVZ (4.33 km/s at 180 km depth). A second LVZ was located directly beneath the Moho, till a depth of 90 km. Since a negative velocity gradient in the lid is not consistent with the observation of S_n-phases in Western Europe up to at least 10 degrees, V_s was averaged down to a depth of 90 km (4.43 km/s). The rise at 120 km could not be drawn into the averaging without seriously affecting the fit to the data.

One of the easiest ways to quantify the fit of a model to the data is by means of the relative residuals, i.e. the difference between the observed and the calculated values for the data divided by the standard error. I will denote the

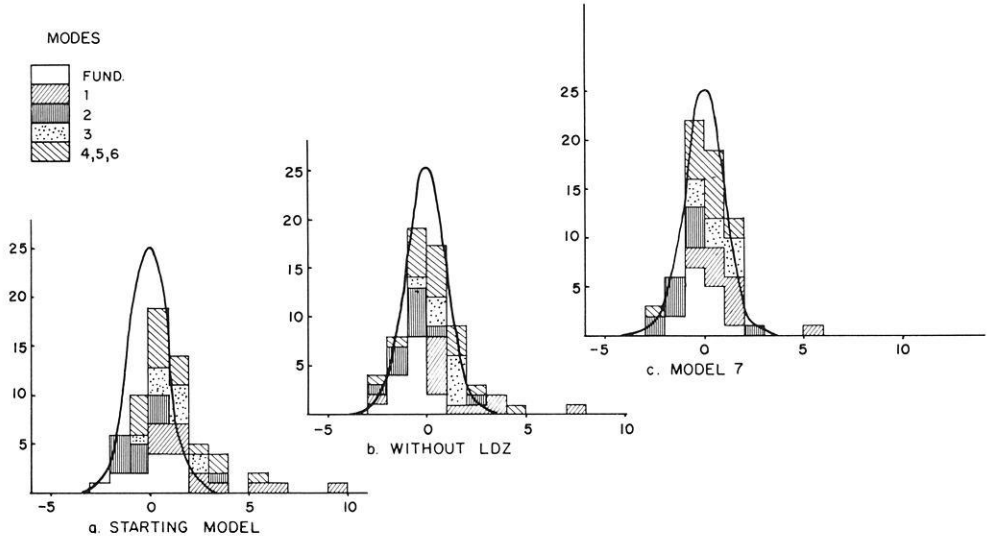

Fig. 8a–c. Histograms showing the distribution of relative residuals of the data computed for 3 different models. A positive residual means that the measured value of the phase velocity is higher than the value that is computed for the model. The solid line is the error curve for the normal distribution

root mean square value of these relative residuals by a quantity ξ. The value of ξ for the starting model is 2.3, which is already considerably better than some of the existing models: for KA-100 (Seidl, 1971) $\xi = 3.0$, and the model SW-Europe, based on data obtained near the Alps, has $\xi = 4.7$.

For normally distributed data with uncorrelated errors, one should aim at a model with $\xi = 1$. If a lower ξ is obtained it may be that one is adjusting the details of the model to the errors rather than to the trend of the data, or that standard errors have been overestimated. If ξ cannot be brought down to 1 the model assumptions may be inadequate or the standard errors have been underrated.

By changing the shear velocity the fit to the data was improved considerably, as can be seen by comparing Figure 8a and b. This way ξ was lowered to a value of 1.7. Some experimenting showed that it can be brought down to 1.6 by introducing more detail but it is impossible to bring ξ close to 1. Inspection of Figure 8b shows that the calculated values for the fundamental and the second higher mode are for almost all periods too high, while those for mode 1 and 3 are in general too low. This bias cannot be removed by changing only the shear velocity, since these variational parameters are everywhere positive (Fig. 9). This means that if we raise the low values for mode 1 and 3 the residuals for mode 0 and 2 will become larger.

Since the compressional velocity has a negligible influence upon the higher modes, the density model has to be responsible for this bias. Therefore, the inversion program was modified to include density perturbations. Unfortunately the limited computer memory did not allow for a joint inversion of density and shear velocity within the framework of the present program.

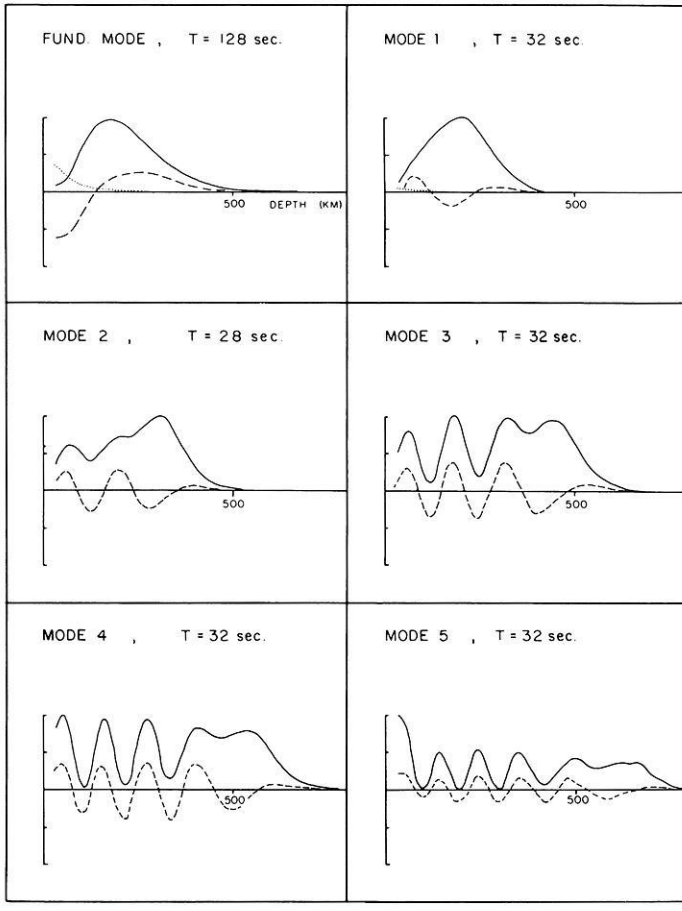

Fig. 9. Variational parameters for the phase velocity of Rayleigh wave modes with respect to perturbations in the shear wave velocity (solid line), compressional wave velocity (dotted line) and density (dashed line) as a function of depth, beneath the crust. The curves for each mode are normalized to an arbitrary scale for units km/sec resp. g/ccm

It is a common misunderstanding to think that phase velocities of surface waves are very insensitive to density perturbations. The cause of this is probably the fact that these phase velocities are indeed unchanged by constant relative density perturbations $\delta\rho/\rho$, because the variational parameters for ρ (keeping the velocities constant) are proportional to the product of ρ^{-1} and the Lagrangian density (Gilbert, personal communication; Nolet, 1976). The variational parameters for the density oscillate, and when multiplied with the density they will give 0 on integration over depth (Fig. 9). But the parameters themselves are in magnitude only slightly smaller than those for the shear velocity, and the phase velocities are in fact rather sensitive to the *detail* in the density model.

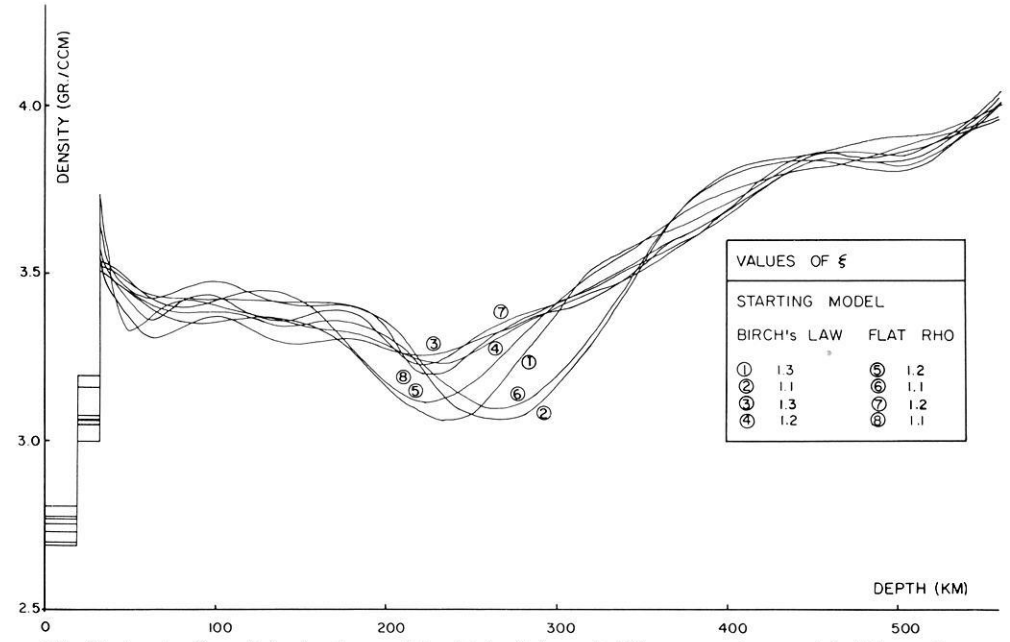

Fig. 10. A set of possible density models obtained from 2 different starting models. The various models were obtained by varying the number of eigenvectors with which the $\rho(r)$-correction is built up in the Backus-Gilbert inversion (models 1, 2, 5 and 6) or by weighting the contribution of each eigenvector in such a way that the largest correction did not exceed a certain bound (models 3, 4, 7 and 8)

To get an impression of the kind of density model that is needed to fit the data I have tried two different starting models (one with constant density and one with ρ varying according to Birch's law in the upper part of the mantle) and several different cut-off criteria for the eigenvectors that participate in the Backus-Gilbert inversion. The results are shown in Figure 10.

Some of these models have a density drop as large as 0.30 g/ccm. Since it was first tried to fit the data with a perturbation in the shear velocity, the density perturbations shown are limited to the perturbations that cannot be traded off against a correction of the shear velocity curve. Model 7 in Figure 10 has a reasonably small density drop (from an average of 3.40 in the lid to 3.29 g/ccm in the zone between 190 and 270 km depth). With this density model ξ can be brought down to 1.2. There does not seem a need to bring ξ further down since we would probably rely too much on the error estimates of the data: if a minimum of 0.02 km/s is imposed on the standard errors in the data, ξ will be exactly 1.0 for model 7. The choice of model 7 among the suite of models shown in Figure 10 is a conservative one in the sense that it is the model with the smallest density drop that still fits the data.

The final result of the inversion procedure is shown in Figure 11. A listing of the model can be found in Table 3. The model seems to be mainly determined by the more precise data among the fundamental and the first and second higher modes.

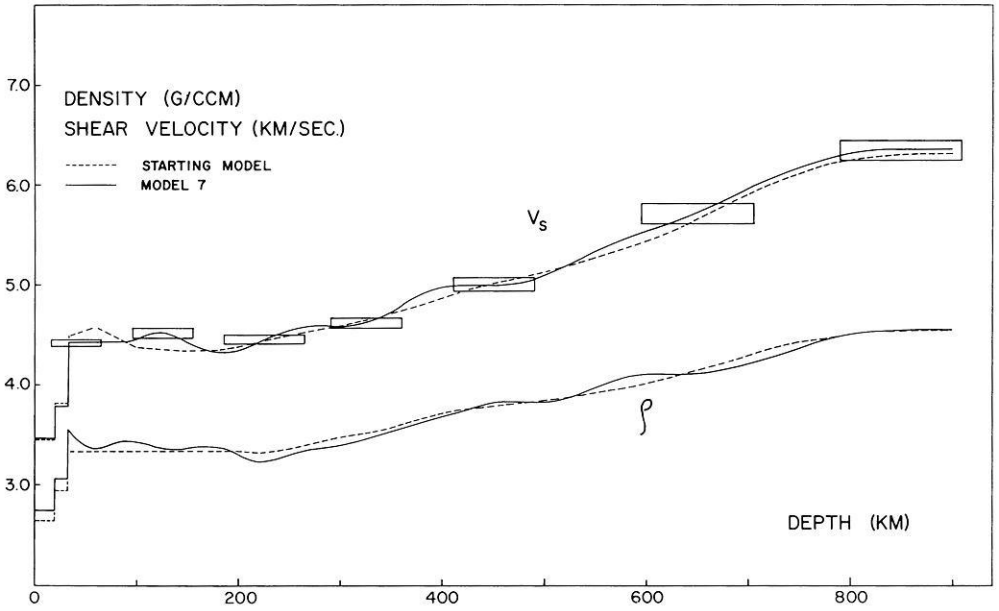

Fig. 11. Plot of the density and shear wave velocity of model 7. Representative points on the trade-off curves for β are shown by boxes with a length s and a height ε: ondulations with a wavelength longer than s and an amplitude larger than ε are warranted by the data. A similar estimate of the uncertainty in ρ has not been determined, but the resolving lengths for ρ are probably larger than those for β

Table 3. Model 7[a]

Depth (km)	V_p (km/s)	V_s (km/s)	Density (g/ccm)	Depth (km)	V_p (km/s)	V_s (km/s)	Density (g/ccm)
0–20	6.000	3.470	2.751	260	8.286	4.585	3.336
20–33	6.700	3.790	3.064	270	8.352	4.593	3.360
33	8.150	4.430	3.555	280	8.418	4.601	3.376
40	8.150	4.430	3.482	290	8.484	4.595	3.387
50	8.150	4.430	3.392	300	8.550	4.592	3.403
60	8.150	4.430	3.363	320	8.673	4.621	3.453
70	8.105	4.430	3.382	340	8.796	4.685	3.510
80	8.060	4.430	3.417	360	8.919	4.798	3.578
90	8.030	4.430	3.439	380	9.031	4.910	3.622
100	8.000	4.454	3.435	400	9.130	4.982	3.682
110	7.965	4.502	3.410	420	9.217	4.994	3.754
120	7.930	4.522	3.381	440	9.303	4.998	3.820
130	7.895	4.515	3.362	460	9.372	5.008	3.844
140	7.860	4.479	3.360	480	9.440	5.039	3.837
150	7.880	4.432	3.371	500	9.516	5.112	3.833
160	7.900	4.390	3.387	540	9.686	5.293	3.937
170	7.930	4.353	3.395	580	9.886	5.458	4.082
180	7.960	4.329	3.382	620	10.123	5.599	4.114
190	8.000	4.333	3.352	660	10.420	5.771	4.128
200	8.040	4.347	3.310	700	10.735	5.970	4.223
210	8.076	4.388	3.238	740	10.989	6.143	4.358
220	8.112	4.430	3.231	780	11.166	6.267	4.471
230	8.148	4.478	3.243	820	11.271	6.343	4.540
240	8.184	4.521	3.270	860	11.306	6.367	4.563
250	8.235	4.555	3.306	900	11.299	6.356	4.561

Linear interpolation has been applied between specified points

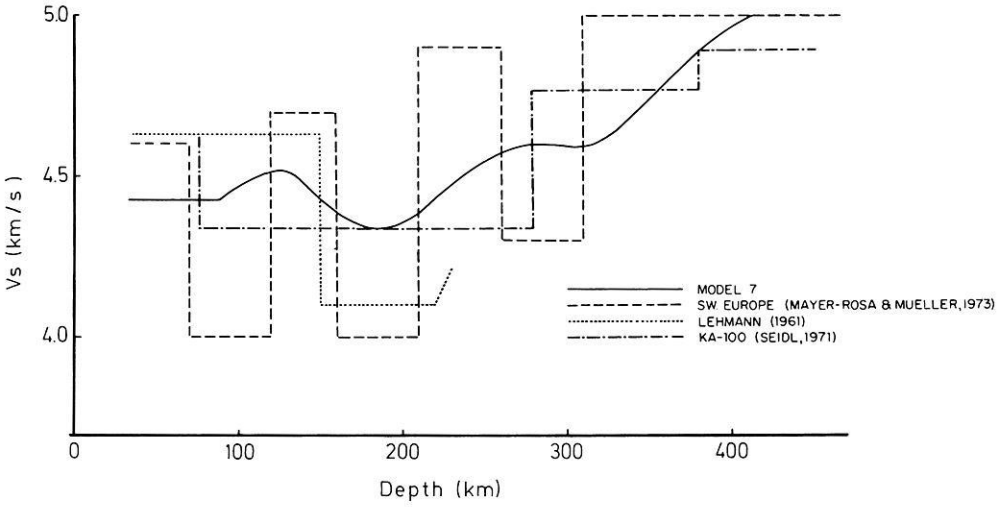

Fig. 12. The shear wave velocity model resulting from this study (model 7) compared with other models proposed for Western Europe

6. Discussion

The resulting model for the shear velocity shows that a value of 4.4–4.5 km/s in the lid is compatible with the fundamental mode phase velocities, so it has been shown that there need not be a discrepancy between S_n-values measured from body-waves and lid velocities inferred from surface wave studies. As most of the details in the shear velocity curve have wavelengths longer than the resolving length (length of the boxes in Fig. 11) and amplitudes larger than the uncertainties (height of the boxes) they should be considered real. There is a rise in V_s before the start of the LVZ. The LVZ is rather shallow and starts at a depth of about 150 km, in accordance with findings by Lehmann (1961), who argues that the LVZ should be located deeper than the depth of some Rumanian earthquakes at 130 km. There is disagreement with the depth of 76 km reported by Seidl (1971) for the model KA-100. The reason is probably that this model was sorted out from a set of Hedgehog models after constraining the thickness of the lithosphere to 70 ± 20 km.

It is interesting to compare the model with the model SW-Europe found by Mayer-Rosa and Mueller (1973) from body and surface wave data (Fig. 12). The rise in model 7 between 100 and 150 km coincides with a zone of high velocity between 120 and 160 km for the model SW-Europe. A low velocity zone between 70 and 120 km as in this model is not excluded by the data set although it is probably possible to fit body wave arrivals with a simple rise near 100 km depth. The third LVZ in the model SW-Europe coincides with a zone of stationary velocity at 300 km in model 7. A full comparison between the models cannot be made as the model SW-Europe is representative for the region near the Alps, and hence based on a different curve for the fundamental Rayleigh

mode. But the bad fit against the higher modes indicates that the velocity contrasts in this model are too large.

On the other hand, from the nature of the inversion problem studied here, sharp discontinuities in the Earth are smoothed out in model 7. The "400 km discontinuity", however, which is only a smooth rise in the starting model, is seen by the higher modes, which have introduced a stronger velocity gradient near 360 km. A second large velocity gradient at a depth of 520 km is less pronounced but coincides with a jump at 540 km that was introduced in the model SW-Europe on the basis of *S*-arrivals at distances between 20 and 25 degrees, and is probably real.

A comparison with recent long-range profile experiments in Western-Europe shows that strong *P*-wave gradients near 90 km (Hirn et al., 1973) and 220 km (Steinmetz et al., 1974) coincide roughly with the *S*-velocity gradients in model 7.

In summary we can say that the upper mantle under Western Europe consists of a shallow LVZ with a minimum V_s of 4.33 km/s between 150 and 230 km depth, preceded by a rise in velocity around 120 km. The strong velocity gradient known as the "400 km discontinuity" and possibly related to the olivine-spinel phase transition is found at a depth of 360 ± 20 km and preceded by a plateau of constant or even decreasing V_s.

Although small-scale details in the density curve are probably not real (Fig. 11), and the height of the curve may be changed by constant amounts $\delta\rho/\rho$, in broad outline we can say that the density drops with at least 0.1 g/ccm when we go from 80 to 220 km depth.

It should be noted here that the possible existence of a layer of anisotropy has been neglected. Calculations for an isotropic Earth show that the ellipticities of the first and second higher mode are of the same order, indicating a similar movement near the surface where most of the anisotropy is supposed to be located (Crampin, 1967). The effects of anisotropy are closely linked to the particle movements, and if the movements calculated for an isotropic Earth are indicative for the movements in a slightly anisotropic one, the effects of anisotropy on the phase velocity could not be of opposite sign for the first and second mode. Moreover, the movement of the third higher mode changes from retrograde to prograde at a period of 43 s, but the experimental phase velocity remains high at this point, as for higher and lower periods. Although we cannot rule out a systematic influence of anisotropy, it is improbable that the low density layer can be traded off against a layer of anisotropic rocks.

Very recently it was pointed out by Randall (1976), Hsi-Ping-Liu et al. (1976) and Anderson and Hart (1976) that the effects of absorption on the normal mode frequencies may not be negligible. An investigation of the effects of anelasticity on the dispersion of the data set used in this study has been started.

But even if anelasticity can result in large phase velocity corrections of different sign for different modes this does not rule out the possible existence of a LDZ. On the basis of quite different data sets both Press (1968, 1970, 1972) and Anderson and Hart (1976) conclude that a LDZ with a drop of 0.1 g/ccm or more is present at depths around 220 km.

This raises some difficult questions as to the cause of a LDZ. It is not the object of this paper to deal with this problem at length. It should be pointed out,

however, that a density drop of this order can never be the result of the temperature rise with depth only. For, according to the Adams-Williamson equation:

$$\frac{d\rho}{dr} = -\rho g \phi^{-1} \tag{5}$$

where $\phi = v_p^2 - \frac{4}{3} v_s^2 \approx 3.7 \times 10^7 \mathrm{m}^2/\mathrm{s}^2$, $g \approx 10\,\mathrm{m/s}^2$ and $\rho \approx 3.4\,\mathrm{g/ccm}$, the density should rise 0.001 g/ccm for each km depth or 0.14 g/ccm from 80 to 220 km depth. Thus the superadiabatic temperature gradient should explain a density drop of 0.25 g/ccm.

Taking the volume expansion coefficient α_v equal to $4 \times 10^{-5}/°\mathrm{C}$ this implies a superadiabatic temperature rise of

$$\Delta T_s = \frac{\Delta \rho}{\alpha_v \cdot \rho} = 1840\,°C. \tag{6}$$

The adiabatic temperature curve increases with only 40 °C over this distance. If the temperature at 80 km is estimated rather low at 620 °C this means a temperature of 2500 °C at 220 km, which by far exceeds the melting point of pyrolite (1700 °C) and other minerals at that depth.

We are therefore forced to conclude that a chemical or mineralogical stratification exists in the upper 300 km of the mantle. If the choice of mantle material is limited to eclogite and peridotite and their mixtures (Clark and Ringwood, 1964) there is no solid-solid phase transition that could be crossed by the geotherm from the heavy to the light phase with increasing depth. Phase transition curves for peridotite are given by Green and Ringwood (1970) and for eclogite by Ito and Kennedy (1971).

One way out of this contradiction would be to suppose that the partial melting in the LVZ leads to a chemical differentation by means of the fractionation of eclogite. This fractionation mechanism was originally proposed by Press (1969) as a possible cause of a LDZ below ocean ridges and makes use of the solid-liquid phase transition of eclogite: the eclogite that is present in the asthenosphere is the source of basaltic melt. This melt, which is lighter and more mobile than the solid material (presumably olivine) migrates upward, where it cools and solidifies into eclogite which has a high density of 3.55 g/ccm. In course of time the cap becomes more and more eclogitic, leaving a peridotite or dunite residue at depth.

Acceptance of this fractionation as a worldwide phenomenon would have consequences for current theories about the mechanism of continental drift (e.g. Jacoby, 1970; Elzasser, 1971; Vlaar, 1975) in the sense that the phase transformation (liquid)basalt/(solid)eclogite cannot be handled as a mere sideshow in the earth's efforts to get rid of its surplus calories.

The energy which is stored as potential energy in the high-density cap is once more released as heat by friction when the lithosphere becomes too heavy and sinks. That the sinking of the lithosphere can be explained purely by gravitational instability was recently demonstrated by Vlaar and Wortel (1976). If the fractionation of eclogite continues far from the ridges, as proposed here, we expect that the thickness of the high-density cap will increase with distance to

the ridge. As the LVZ gets depleted the velocity contrast will diminish. Thus, the differences found for LVZ's under continents and oceans may partly be of chemical origin. At the same depths the pressure will be higher in the older parts of the asthenosphere, causing a flow of material towards younger parts. Hence. the counterflow of material at depth that is necessary for any convective mechanism may very well be located in the asthenosphere. This conclusion differs from that reached by Schubert and Turcotte (1972).

Acknowledgements. I am indebted to Professor N.J. Vlaar for his guidance throughout the course of this work, and to Professor F. Gilbert for stimulating discussions in the initial stages of this research. The discussions and comments provided by Rinus Wortel and other collegues at the Vening Meinesz Laboratory are gratefully acknowledged. Dr. A.R. Ritsema and Joost Vermeulen were helpful in selecting and obtaining seismograms. Professor M. Båth and Dr. S.E. Johnstad kindly put recordings of their stations at my disposal. Giuliano Panza helped in the writing of the stacking program. This research was supported by the Netherlands Organisation for the Advancement of Pure Research (Z.W.O.).

References

Alterman, Z.: Higher-mode surface waves. In: The earth's crust and upper mantle, P.J. Hart, ed., 265, A.G.U., Washington D.C. 1969

Anderson, D.L., Hart, R.S.: An earth model based on free oscillations and body waves. J. Geophys. Res. **81**, 1461, 1976

Backus, G., Gilbert, F.: Uniqueness in the inversion of inaccurate gross earth data. Phil. Trans. Roy. Soc. London Ser. A **266**, 123, 1970

Båth, M.: Average crustal structure of Sweden. Pure Appl. Geophys. **88**, 75, 1971

Cara, M.: Observations d'ondes Sa de type SH. Pure Appl. Geophys. **114**, 141, 1976

Clark, S.P., Ringwood, A.E.: Density distribution and constitution of the mantle. Rev. Geophys. **2**, 35, 1964

Crampin, S.: Higher modes of seismic surface waves: Phase velocities across Scandinavia. J. Geophys. Res. **69**, 4801, 1964

Crampin, S.: Coupled Rayleigh-Love second modes. Geophys. J. **12**, 229, 1967

Der, Z.A., Landisman, M.: Theory for errors, resolution and separation of unknown variables in invers problems, with applications to the mantle and crust of Southern Africa and Scandinavia. Geophys. J. **27**, 137, 1972

Dziewonski, A.M., Hales, A.L.: Numerical analysis of dispersed seismic waves. Methods in Computational Physics **11**, 39, 1972

Elzasser, W.M.: Sea floor spreading as thermal convection. J. Geophys. Res. **76**, 1101, 1971

Fagerness, V., Kanestrom, R.: Variations in upper mantle structure as derived from Pn and Sn waves. Pure and Appl. Geophys. **109**, 1762, 1973

Forsyth, D.W.: A new method for the analysis of multi-mode surface wave dispersion: Application to Love wave propagation in the East Pacific. Bull. Seism. Soc. Am. **65**, 323, 1975

Gilbert, F.: Ranking and winnowing gross earth data for inversion and resolution. Geophys. J. **23**, 125, 1971

Gilbert, F., Dziewonski, A.M.: An application of normal mode theory to the retrieval of structural parameters and source mechanisms from seismic spectra. Phil. Trans. Roy Soc. London **278**, 187, 1975

Green, D.H., Ringwood, A.E.: Mineralogy of peridotite compositions under upper mantle conditions. Phys. Earth Planet. Interiors **3**, 359, 1970

Hirn, A., Steinmetz, L., Kind, R., Fuchs, K.: Long range profiles in W. Europe: II. Fine structure of the lower lithosphere in France (Southern Bretagne). Z. Geophys. **39**, 363, 1973

Hsi-Ping Liu, Anderson, D.L., Kanamori, H.: Velocity dispersion due to anelasticity; implications for seismology and mantle composition. Geophys. J. 1976, in press

Ito, K., Kennedy, G.C.: An experimental study of the basalt-garnet granulite-eclogite transition. In: The structure and physical properties of the earth's crust, J.G. Heacock, ed. Geophys. Monogr. Ser. **14**, Washington 1971

Jackson, D.D.: Interpretation of inaccurate, insufficient and inconsistent data. Geophys. J. **28**, 97, 1972

Jacoby, W.R.: Instability in the Upper Mantle and global plate movements. J. Geophys. Res. **75**, 5671, 1970

Knopoff, L.: Observation and inversion of surface wave dispersion. Tectonophysics **13**, 497, 1972

Kovach, R.L.: Seismic surface waves: Some observations and recent developments. Phys. Chem. Earth **6**, 251, 1965

Lehmann, I.: *S* and the structure of the upper mantle. Geophys. J. **4**, 124, 1961

Mayer-Rosa, D., Mueller, St.: The gross velocity depth distribution of P and S waves in the upper mantle of Europe from Earthquake observations. Z. Geophys. **39**, 395, 1973

Mendiguren, J.A.: Identification of free oscillation spectral peaks for 1970 July 31, Colombian deep shock using the excitation criterion. Geophys. J. **33**, 281, 1973

Nolet, G.: Higher Rayleigh modes in Western Europe. Geophys. Res. Letters **2**, 60, 1975

Nolet, G.: Higher modes and the determination of upper mantle structure. Ph.D. thesis, Utrecht 1976

Nolet, G., Panza, G.F.: Array analysis of seismic surface waves: Limits and possibilities. Pure Appl. Geophys. **114**, 775, 1976

Payo, G.: Crustal phases across the Iberian Peninsula region. Ann. di Geophys. **17**, 523, 1964

Payo, G.: Iberian peninsula crustal structure from surface wave dispersion. Bull. Seism. Soc. Am. **55**, 727, 1964

Press, F.: Earth models obtained by Monte Carlo inversion. J. Geophys. Res. **73**, 5223, 1968

Press, F.: The suboceanic mantle. Science **165**, 174, 1969

Press, F.: Earth models consistent with geophysical data: Phys. Earth Planet. Interiors **3**, 3, 1970

Press, F.: The earth's interior as inferred from a family of models. In: The nature of the solid earth, E.C. Robertson, ed. New York: McGraw-Hill 1972

Randall, M.J.: Attenuative dispersion and frequency shift of the earth's free oscillations. Phys. Earth Planet. Interiors **12**, P1, 1976

Sapin, M., Prodehl, C.: Long Range profiles in Western Europe I—crustal structure between Bretagne and the central Massif of France. Ann. Geophys. **29**, 127, 1973

Schubert, G., Turcotte, D.L.: One-dimensional model of shallow-mantle convection. J. Geophys. Res. **77**, 945, 1972

Seidl, D.: Spezielle Probleme der Ausbreitung Seismischer Obenflächenwellen mit Beobachtungsbeispielen aus Europa. Thesis, Karlsruhe 1971

Steinmetz, L., Hirn, A., Perrier, G.: Réflexions séismiques à la base de l'asthénosphére. Ann. Geophys. **30**, 173, 1974

Vlaar, N.J.: The driving mechanism of plate tectonics: a qualitative approach. In: Progress in geodynamics, G.J. Borradaile et al., eds. Amsterdam 1975

Vlaar, N.J., Wortel, R.: Lithospheric aging, instability and subduction. Tectonophysics **32**, 331, 1976

Wiggins, R.A.: The general linear inverse problem: implication of surface waves and free oscillations for earth structure Rev. Geophys. Space Phys. **10**, 251, 1972

Received October 1, 1976